PCCP
Physical Chemistry Chemical Physics

Accepted Manuscript

This article can be cited before page numbers have been issued, to do this please use: C. S. Lehmann and K. Weitzel, *Phys. Chem. Chem. Phys.*, 2020, DOI: 10.1039/D0CP01376E.

ROYAL SOCIETY OF CHEMISTRY

rsc.li/pccp

View Article Online
DOI: 10.1039/D0CP01376E

ARTICLE

Coincident measurement of photo-ion circular dichroism and photo-electron circular dichroism

Received 00th January 20xx,
Accepted 00th January 20xx

DOI: 10.1039/x0xx00000x

Carl Stefan Lehmann and Karl-Michael Weitzel *[a]

Two methods of laser-induced mass-selective chiral analysis based on circular dichroism have been reported in literature: photo-ion circular dichroism (PICD) and photo-electron circular dichroism (PECD). In PICD, a difference in total ion yields upon multiphoton ionization with circular polarized light is measured, whereas in PECD the circular dichroism is observed in the angular distribution of the photoelectrons. Here we report the first coincident measurement of the PICD and PECD effect. A home-built photoion-photoelectron coincidence spectrometer has been used to measure both the PICD and the PECD effect simultaneously under the same measurement conditions. Pure samples of R- and S-Methyloxirane have been photo-ionized using a femtosecond laser operation at 396 nm.

Introduction

Chiral identification techniques, that can probe the handedness of a chiral molecule, are of great importance in analytical chemistry and pharmacy, since chiral molecules often have pharmacological or biological properties different for the enantiomers. Since the physical and chemical properties of enantiomers are similar, experimental possibilities for analysis and distinction are limited to such techniques that are sensitive to the chirality.

Chemical techniques for chirality analysis include diastereomer formation in the interaction of two chiral molecules, which is e.g. the basis for chiral chromatography.[1,2] The absolute configuration of enantiomers can be determined e.g. by fs-laser or beam foil collision induced Coulomb explosion [3,4]. Physical techniques, on the other hand, include the class of chiroptical methods. This class can be further subdivided into approaches using linear polarized light and others using circular polarized light. Into the former class, belongs the classical technique of optical rotation dispersion[5]. Phase-sensitive microwave spectroscopy has been demonstrated to be a powerful approach for the analysis of chiral isomer mixtures.[6,7] The current work deals with a technique employing circular polarized light. Here, the classical approach is measuring the circular dichroism (CD) given by the difference in extinction coefficients, ε, of chiral molecules for left-handed circular polarized light (LCP) and right-handed circular polarized light (RCP).[8] Classically, the CD effect is measured in one photon absorption and quantified by the anisotropy factor *g*:

$$g = 2 \cdot \left(\frac{\varepsilon_{LCP} - \varepsilon_{RCP}}{\varepsilon_{LCP} + \varepsilon_{RCP}} \right) \quad (1)$$

However, CD is limited to measurements in solution since the signals are rather weak. CD spectra in solution are in general broad and not sensitive to chemical impurities. To analyse the composition of a sample, CD is often coupled to other analysing techniques, such as chromatography or mass-spectrometry.

In recent decades, more sophisticated methods, that look at enantioselective, chiroptical excitation in ionization, have been developed: photoion circular dichroism (PICD) and photoelectron circular dichroism (PECD). The signal strengths of both PICD and PECD can be up to tens of percent – more than 3-4 orders of magnitude larger than conventional CD.

In PICD, a sample is ionized in the source of a mass spectrometer using a multiphoton ionization process. The PICD effect is measured as the difference in the ionization yield[9]:

$$PICD = 2 \cdot \left(\frac{Y_{LCP} - Y_{RCP}}{Y_{LCP} + Y_{RCP}} \right) \quad (2)$$

Where Y_{LCP} and Y_{RCP} are the ionization yields of a specific ion upon ionization with LCP and RCP, respectively. In general laser ionization is accompanied by a certain fragmentation pattern. For each fragment ion considered there is a specific PICD value. The PICD effect inverts upon switching the enantiomer. The first PICD experiments were reported using ns-lasers.[10–12] Later Weitzel and co-workers extended the method to fs-laser ionization.[13–16] Mass selective chiral analysis studies have been recently reviewed.[17]

Any single ionization event leads to the formation of one cation and one electron. Consequently the information contained in total electron yields must be the same as that contained in total ion yields. However, the chirality information of a molecule is also contained in the asymmetry of the photoelectron angular

[a] Fachbereich Chemie, Philipps-Universität Marburg, 35032 Marburg, Germany. Email: weitzel@chemie.uni-marburg.de

Electronic Supplementary Information (ESI) available: [details of any supplementary information available should be included here]. See DOI: 10.1039/x0xx00000x

distribution with respect to the laser propagation direction. This asymmetry is commonly referred to as PECD defined by[18]

$$PECD = 2 \cdot \left(\frac{Y_{LCP,f} - Y_{LCP,b}}{Y_{LCP}} - \frac{Y_{RCP,f} - Y_{RCP,b}}{Y_{RCP}} \right)$$
$$= 4 \cdot \left(\frac{Y_{LCP,f} - Y_{LCP,b}}{Y_{LCP}} \right) \quad (3)$$
$$= -4 \cdot \left(\frac{Y_{RCP,f} - Y_{RCP,b}}{Y_{RCP}} \right)$$

with

$$Y_{LCP} = Y_{LCP,f} + Y_{LCP,b}$$
$$Y_{RCP} = Y_{RCP,f} + Y_{RCP,b}$$

where, for example, $Y_{LCP,f}$ stands for the total electron yield in the forward direction measured with LCP.

The PECD effect was theoretically predicted by Richtie[19] in 1976. However, it were the theoretical papers by Powis[20,21] in 2000 that have stimulated/activated the PECD research field. Recently, the theoretically description of PECD was extended to the multiphoton regime.[22,23]

The first (single photon) PECD experiment was reported in 2001 by Böwering *et al*. using synchrotron radiation.[24] In the last decade, the first laser (multiphoton) PECD studies[18,25] were reported. Mass-selective PECD can be achieved using photoelectron-photoion coincidence spectrometers and this was applied for the analysis of multicomponent mixtures.[26] Besides, it was demonstrated that PECD is even present in the strong field regime (ATI and tunnel ionization).[27,28] Studies have shown that PECD is sensitive to the initial orbital from which the electron is ejected[29], the molecular conformation[30] as well as the molecular orientation.[31] Furthermore, it has been shown that the ellipticity of the laser pulse can provide an additional dimension to discriminate enantiomers. [32–34]

The total transition dipole moment for the interaction of a molecule with electro-magnetic radiation consists of electric dipole contributions, magnetic dipole contributions and higher order terms.[35] Conceptually, PICD and PECD arise from different contributions to the total transition dipole moment. For the multiphoton excitation considered in this work the PICD arises from the magnetic dipole transition in the multiphoton excitation. Its characteristics is in general dominated by the initial resonant photon absorption.[10,14,36] The PECD, on the other hand, arises from the scattering of the electron in the chiral molecular potential of the final ionization step due to a purely electric dipole effect.[37]

The observed PECD signal depends on details of the (multiphoton) nature of an ionization process. For example, in Camphor the observed multiphoton PECD is increased due to the 3rd order legendre polynomial, b_3, (opposite sign with respect to the first order, b_1)[18,25], while in Fenchone the measured b_1 and b_3 had the same sign leading to a net decrease of the observed PECD.[2] In MeOx the net effect of the higher order legendre polynomials on the PECD was close to zero.[38]

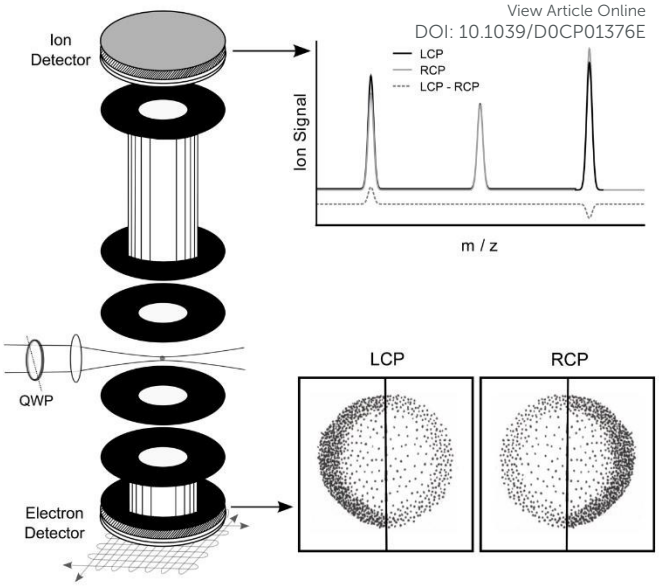

Fig. 1: On the left, a schematic of the experimental setup is shown. Laser pulses with a central wavelength of 396 nm are focused into the photoion-photoelectron coincidence spectrometer. After ionization of a molecule, the electron and the ion were detected in coincidence on the two opposite detectors. The electron detector measures the mass-tagged photoelectron angular distributions (artist view, bottom right) from which the PECD is calculated. The ion detector records the time-of-flight of the coincident ion (top right). The PICD is calculate from the difference in absolute yields for ionization with LCP and RCP.

Therefore, PICD and PECD experiments can complement each other. For example, a molecule can have a strong PICD signal but low PECD signal or vice versa. Ideally, both PECD and PICD should be measured simultaneously using photoelectron-photoion coincidence, as it could provide an additional discrimination for identifying components in mixtures of compounds.

The femtosecond laser photoelectron photoion coincidence technique has been pioneered by Davies *et al*.[39] and Stert *et al*.[40] Unfortunately, in all PECD experiment published to date, even in coincidence measurements, the PICD effect has been cancelled out by normalization of the data. Whereas, all the published PICD experiments were performed in non-coincidence spectrometers. Thus, it is currently not possible to say whether a de facto exclusion exists between PECD and PICD.

In this paper, we report the coincidence measurement of both PICD and PECD of Methyloxirane (MeOx) upon fs-multiphoton ionization at 396 nm in a single experiment.

Experimental Section

The experimental photoelectron-photoion coincidence spectrometer is schematically shown in Fig. 1. After ionization of a molecule, the electron and the ion were detected in coincidence on the two opposite detectors. A time- and position-sensitive delay line detector (Roentdek DLD40) was used to measure the electron, whereas the ion time-of-flight was measured with two chevron-stacked microchannel plates in combination with a copper anode (no position information). Constant voltages, optimized for electron imaging resolution,

were applied on the electrostatic lenses, leading to an electric field of 200 V cm^{-1} in the ionisation region. The use of constant voltages limits our mass resolution to m/Δm = 120. Higher ion mass resolution in combination with a high electron imaging resolution could be achieved by switching the voltages on the electrostatic lenses.[41]

Both enantiomers of MeOx were purchased from Alfa Aesar and had a purity of 99%. The samples are effusively introduced into the vacuum chamber via 2 separate gas lines. The typical pressure inside the ionization chamber was 1 x 10^{-5} mbar. The pressure fell to below 5 x 10^{-8} mbar in between switching the enantiomers.

Femtosecond laser pulses with a central wavelength of 792 nm and a pulse duration of 30 fs were generated by a Ti:Sapphire multipass amplifier system with a repetition rate of 15 kHz and an average output power of 7 W (Dragon, KMLabs). A fraction of the output beam was subsequently frequency doubled in a 200 µm thick BBO crystal. The frequency double spectrum had a central wavelength of 396.0 nm and a spectral bandwidth of 7.3 nm. Two dichroic mirrors were used to separate the second harmonic from the fundamental beam. The SHG beam was focused down to a spot size of 100 µm x 70 µm. Due to the dispersion of the optical elements, the estimated maximum pulse duration in the ionisation chamber is 90 fs.

The laser intensity was continuously monitored by a power meter located behind the coincidence spectrometer, i.e. behind the output window. The experiments were performed with a pulse energy of 0.7 ± 0.1 µJ. The resulting intensity in the ionization volume is estimated to be 10^{11} W cm^{-2}. Under these measurement conditions, approximately 0.027 for electrons, 0.027 ions and 0.01 coincidence events were detected per laser shot. This results in a total ionization rate of 0.07 ionized molecules per laser shot[42], therefore limiting the probability of false coincidence to less than 0.1% according to Poisson statistics.

The circularly polarized light was generated by an achromatic broadband quarter-waveplate (RAC 2.4.15, B-Halle). The quality of the CPL was analysed before and after the measurement. The circular polarisation of both RCP as well as LCP was ≥97%.

A fast stepper motor was used to rotate the quarter waveplate, switch the handedness of the circular polarized light, every 10 s (150 000 laser shots) in order to reduce effects of any experiment drift.

The total dataset for each enantiomer and handedness contained a total of 54 million laser shots (360 x 10 s). Each coincident event was analysed and categorized as follows: enantiomer (R or S), ion mass, polarisation (LCP or RCP) and depending on the position on the electron detector either as forward (f) or backward (b).

The PECD and PICD was calculated for each small dataset, consisting of consecutive measurements of LCP and RCP. Subsequently the mean value and standard error were calculated from the 360 small measurements.

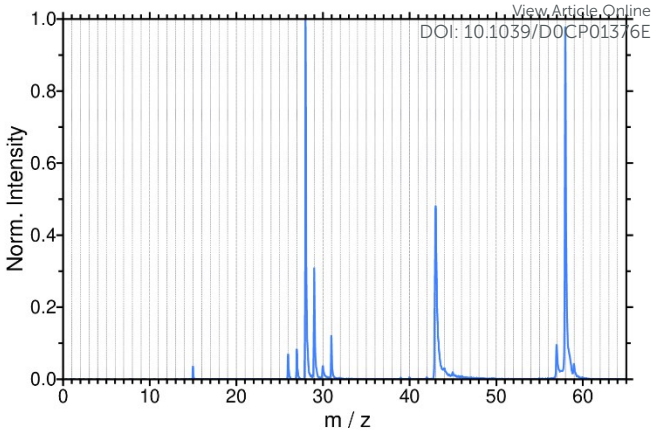

Fig. 2: Typical measured coincident mass spectrum of Methyloxirane. Data from R-Methyloxirne measured with left circular polarized light is shown. Measurements on the other enantiomer and/or other circular polarization yielded the same fragmentation pattern, with minor differences (1-2 %) in the absolute yield of the different ion masses.

Results and Discussion

The typical coincident mass spectrum of MeOx after multiphoton ionization at 396.0 nm is shown in Fig. 2. A rich fragmentation pattern is observed, with the most intense signals belonging to the parent ion (m/z = 58) and the fragment ion with m/z = 28.

The adiabatic ionization energy of MeOx and the appearance energies for the fragment ions were reported by Garcia *et al.*[43] and are listed in Table 1. Four photons at 396.0 nm provide an energy of 12.5 eV, which is enough energy for the formation of most of the ions observed in the mass spectrum. Five photons are required for the formation of the lower mass fragment ions (m/z = 15, 26, 27). Rafiee Fanood *et al.*[38] have measured the multiphoton ionization of MeOx at a slightly higher wavelength of 420 nm. They observed the same ions in their mass spectrum, although with lower fragmentation; that is a higher parent ion yield. This difference in fragmentation is most likely caused by laser characteristics (i.e. spectral bandwidth, chirp, pulse energy), as they optimized their measurement conditions to limit fragmentation.

Table 1 Fragment and parent ions observed in the mass spectrum of Methyloxirane (Fig. 2) and their appearance energies (AE), as well as the number of photons needed for the excitation wavelength of 396 nm.

m/z	Formula	AE (eV)[a]	Photons needed
15	CH_3^+	12.74	5
26	$C_2H_2^+$	13.54	5
27	$C_2H_3^+$	13.04	5
28	$C_2H_4^+$ / CO^+	11.32	4
29	$C_2H_5^+$ / HCO^+	10.88	4
30	$C_2H_6^+$ / H_2CO^+	10.84	4
31	H_3CO^+	10.94	4
43	$C_2H_3O^+$	10.87	4
57	$C_3H_5O^+$	10.67	4
58	$C_3H_6O^+$	10.24	4

[a] data taken from Ref [43]

We will continue by first presenting the results on the photoion circular dichroism, followed by the results obtained for the photoelectron circular dichroism. For the determination of both effects the three dominant peaks in the mass spectrum are used; that is the parent ion (m/z = 58) and the fragment ions with m/z = 28 and m/z = 43. All data discussed in this paper are coincidence data only. We have used all coincidence events; i.e. no selection based on electron kinetic energy was applied for the PICD as well as the PECD determination. We have checked that the PICD values of the coincidence and non-coincidence (all ions) datasets are, within the experiment error, very similar.

PICD

Fig. 3 shows the PICD as a function of mass to charge ratio. The two enantiomers of MeOx can clearly be distinguished: the PICD value of R-MeOx is negative for all ions with an average value of approximately -7%, whilst the PICD is positive for S-MeOx.

The PICD values and their corresponding errors for the different ions are listed in the second column of Table 2. For R-MeOx, the PICD value of parent ion is -7.3 ± 1.1%. The PICD value of the fragment ion with m/z = 28 is -6.8 ± 1.1%, hence close to the PICD value of the parent ion. The PICD value of $C_2H_3O^+$ (m/z = 43) is 1.5% lower than that of the parent ion, i.e. -5.8 ± 1.1%.

For the purpose of presentation and to correct for any systematic errors, the PICD values plotted in Fig. 3 were symmetrized around zero. However, we note that the raw (unsymmetrized) PICD values of all R-MeOx ions were negative and respectively positive for all S-MeOx ions (see Fig. S1 and Table S1 in the ESI). The asymmetries in the PICD values could be corrected by introducing a reference sample[9,13], however this has the disadvantage of the loss of mass information due to overlapping mass signals between sample and reference.

To the best of our knowledge, the only other PICD measurement on MeOx was reported by Horsch *et al*.[13] They measured a PICD value for the parent ion of R-MeOx of +2.2 ± 0.9%, +1.9 ± 1.1% and +0.4 ± 0.5% for the multiphoton excitation at 810 nm, 878 nm and 738 nm, respectively. Unfortunately, they could not report the PICD values for the fragment ion of m/z = 43, as it overlapped with the reference sample.

Under our measurement condition, we observe a larger discrimination of the enantiomers; that is a higher absolute PICD value. This could be attributed to either the positive chirp of the laser pulse in our experiment and/or the excitation wavelength. For example, Horsch *et al*.[15] demonstrated that a longer pulse duration, by applying a positive as well as a negative linear chirp, can increase the PICD value by over a factor of 3. For 3-Methylcyclopentanone a pronounced wavelength dependence of the PICD was also observed, the values being -0.8% at 648 nm[3] and +27% at 324 nm.[12]

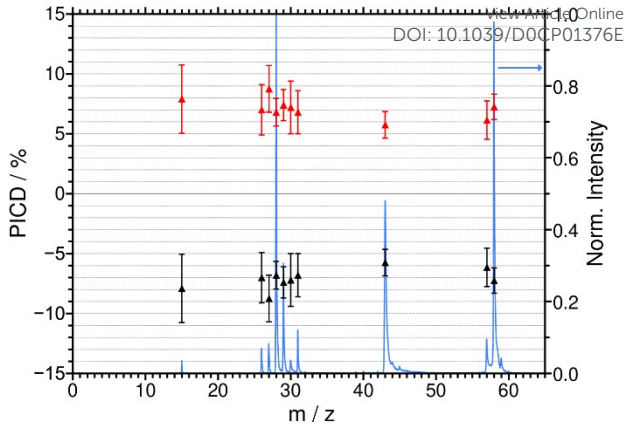

Fig. 3: PICD values, measured in coincidence, for R-Methyloxirane (black) and S-Methyloxirane (red) and the mass spectrum (blue) for the multiphoton excitation at 396.0 nm. The PICD values for R-Methyloxirane are listed in the second column of Table 2.

Table 2: Symmetrized PICD and PECD values and their corresponding standard for the multiphoton excitation of Methyloxirane at 396.0 nm. The sign of the PICD and PECD values corresponds to the value of R-Methyloxirance. The ions that dominant the mass spectrum are highlighted.

m/z	PICD (%)	PECD (%)
15	-7.9 ± 2.9	-6.5 ± 7.9
26	-7.0 ± 2.1	-5.3 ± 5.2
27	-8.8 ± 1.9	-6.8 ± 4.5
28	**-6.8 ± 1.1**	**-8.4 ± 1.4**
29	-7.4 ± 1.3	-6.2 ± 2.3
30	-7.2 ± 2.2	-5.2 ± 5.6
31	-6.8 ± 1.8	-9.0 ± 3.9
43	**-5.8 ± 1.1**	**-7.9 ± 1.5**
57	-6.2 ± 1.6	-6.4 ± 3.7
58	**-7.3 ± 1.1**	**-4.4 ± 1.3**

PECD

The multiphoton PECD as a function of mass to charge ratio is shown in Fig. 4 and the values for R-MeOx are tabulated in the third column of Table 2. To correct for any systematic errors and for the purpose of presentation, the PECD values shown in Fig. 4 and Table 2 were symmetrized around zero. The raw PECD data are listed Table S2 and S3 and are shown Fig S2 (ESI).

It is observed that the PECD values for the different ions of R-MeOx are negative and span the range of -4% to -9%. For R-MeOx, the PECD value of the parent ion is at -4.4 ± 1.3% the lowest PECD value, in absolute terms, of all the detected ions. The PECD values of the fragment ions corresponding to m/z = 28 and m/z = 43 are -8.4 ± 1.4% and -7.9 ± 1.5%, respectively. Hence, both fragment ions have a significantly higher PECD value than the parent ion.

Rafiee Fanood *et al*.[38] have measured the PECD for multiphoton ionization of MeOx at a slightly higher wavelength of 420 nm. For the parent ion of R-MeOx, they reported a mean PECD value

View Article Online
DOI: 10.1039/D0CP01776B

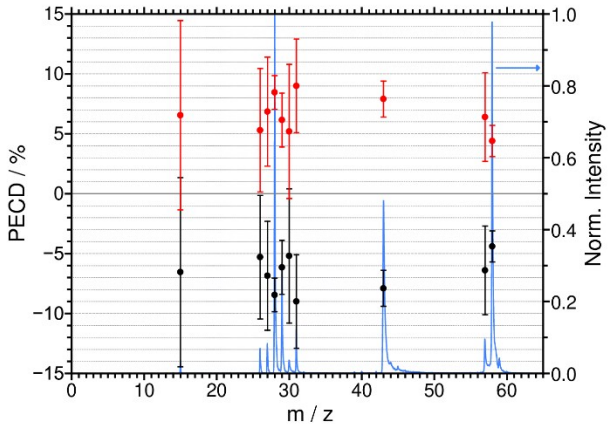

Fig. 4: PECD values, measured in coincidence, for R-Methyloxirane (black) and S-Methyloxirane (red) and the mass spectrum (blue) for the multiphoton excitation at 396.0 nm. The PECD values for R-Methyloxirane are listed in the third column of Table 2.

for electrons associated with photoexcitation from the HOMO-1 orbital of -4.7 ± 0.8%, whilst the selection of electrons associated with the photoexcitation of the HOMO orbital (electrons with higher kinetic energy) resulted in an increased PECD value in the excess of -10%. %. The variation of the PECD over the photoelectron spectrum has also been observed in single-photon PECD measurement.[44]

We also observe an increase in the PECD value of the parent ion of R-MeOX to approximately -8%, when selecting the high kinetic energy electrons. The influence of the kinetic energy of the electrons is illustrated in the supplementary information (Fig. S4). However, since the focus of this paper is on the coincident detection and especially the comparison of PICD and PECD, we have chosen to present the data without the selection of electron kinetic energy.

Overall, the PECD effect observed for the parent ion in this work at 396 nm is slightly smaller than for the multiphoton excitation at 420 nm.[4] For the $C_2H_3O^+$ fragment ion (m/z = 43) this is reserved; under our measurement condition the PECD effect (for R-MeOx) increases to -7.9 ± 1.5%, while the reported PECD effect at 420 nm was close the -4%.[38] We observe an even higher PECD of -8.4 ± 1.4% for the fragment ion with m/z = 28. Since the authors of Ref [38] optimized their experimental conditions to limit fragmentation, they only reported a PECD value for all ions with a mass to charge ratio of 26 to 32. For this range they observed a PECD on the order of -6%.

PICD and PECD comparison

The PICD and PECD effects rely on different selection rules, therefore both measurement techniques can complement each other. It is a priori not always obvious which of these techniques will offer the higher degree of distinguishability for the enantiomers under investigation. This could also change, for example, as a function of ion mass to charge ratio and/or laser characteristics (i.e. wavelength, pulse energy, pulse duration, chirp).

To illustrate this, it is useful to compare columns 2 and 3 of Table 2. Whilst for parent ion of Methyloxirane PICD offers a better distinction than PECD. This is reserved for the two dominant fragment ions (m/z = 28 and 43), that is the measured PECD is greater than the PICD. Furthermore, it is interesting to note that we observe in increase of the PECD value from -4.4% to -8% when selecting the higher kinetic energy electrons of the parent ions (Fig S4 in the ESI). In contrast, the PICD value remains effectively unaltered (-7.3% vs -7.1%) for the same selection (Fig S3 in the ESI).

To understand these differences in behaviour between the measured PICD and PECD values, further investigation are needed. It is needless to say that these studies should be performed under the same measurement, therefore in photoion-photoelectron coincidence experiments.

Conclusions

In this paper, we have presented the first measurements on the distinction of chiral molecules using the PICD and PECD detection techniques in coincidence; that is under the same measurement condition. We have used a photoion-photoelectron coincidence detection in combination with fs-multiphoton ionization at 396 nm to distinguish the enantiomers of the chiral molecule Methyloxirane. For R-Methyloxirane, the PICD as well as the PECD are negative. The parent ion show a higher negative value for PICD than for PECD, but this reverses for the dominant fragment ions (m/z = 28 and 43).

Most likely, it is a pure coincidence that PECD and PICD have an almost identical magnitude and sign in the Methyloxirane studied in this work. In general, this is not expected to be the case. Therefore, the simultaneous detection of both the PICD and PECD would provide complementary information to discriminate chiral molecules. This should lead to a higher chiral selectivity, especially in cases where multicomponent mixtures are analysed.

Clearly, more theoretical work is required to better understand the complementarity of PICD and PECD, in particular considering the wavelength dependence, the role of resonant intermediate states and the duration of the excitation pulse.

Conflicts of interest

There are no conflicts to declare.

Acknowledgements

Financial support of this work from the Deutsche Forschungsgemeinschaft (DFG) under contract no. We 1330 / 19 is gratefully acknowledged.

Notes and references

1. N.R. Srinivas, *Biomed Chromatogr*, 2004, **18**(4), 207.
2. I. Ilisz, R. Berkecz and A. Péter, *J Pharm Biomed Anal*, 2008, **47**(1), 1.

3. M. Pitzer, M. Kunitski, A.S. Johnson, T. Jahnke, H. Sann, F. Sturm, L.P.H. Schmidt, H. Schmidt-Böcking, R. Dörner, J. Stohner, J. Kiedrowski, M. Reggelin, S. Marquardt, A. Schießer, R. Berger and M.S. Schöffler, *Science*, 2013, **341**(6150), 1096.
4. P. Herwig, K. Zawatzky, M. Grieser, O. Heber, B. Jordon-Thaden, C. Krantz, O. Novotný, R. Repnow, V. Schurig, D. Schwalm, Z. Vager, A. Wolf, O. Trapp and H. Kreckel, *Science*, 2013, **342**(6162), 1084.
5. L.D. Barron, *Molecular Light Scattering and Optical Activity,* Cambridge University Press, 2009, 39.
6. D. Patterson, M. Schnell and J.M. Doyle, *Nature*, 2013, **497**(7450), 475.
7. V.A. Shubert, D. Schmitz, D. Patterson, J.M. Doyle and M. Schnell, *Angew Chem Int Ed Engl*, 2014, **53**(4), 1152.
8. Berova N, Nakanishi K, Woody RW, editors, *Circular dichroism*: *Principles and applications,* Wiley-VCH, New York, NY, 2nd ed., 2000.
9. C. Logé, A. Bornschlegl and U. Boesl, *Anal Bioanal Chem*, 2009, **395**(6), 1631.
10. U. Boesl and A. Bornschlegl, *ChemPhysChem*, 2006, **7**(10), 2085.
11. R. Li, R. Sullivan, W. Al-Basheer, R.M. Pagni and R.N. Compton, *The Journal of Chemical Physics*, 2006, **125**(14), 144304.
12. A. Bornschlegl, C. Logé and U. Boesl, *Chemical Physics Letters*, 2007, **447**(4), 187.
13. P. Horsch, G. Urbasch, K.-M. Weitzel and D. Kröner, *Phys Chem Chem Phys*, 2011, **13**(6), 2378.
14. H.G. Breunig, G. Urbasch, P. Horsch, J. Cordes, U. Koert and K.-M. Weitzel, *ChemPhysChem*, 2009, **10**(8), 1199.
15. P. Horsch, G. Urbasch and K.-M. Weitzel, *Zeitschrift für Physikalische Chemie*, 2011, **225**(5), 587.
16. P. Horsch, G. Urbasch and K.-M. Weitzel, *Chirality*, 2012, **24**(9), 684.
17. U. Boesl and A. Kartouzian, *Annual Rev. Anal. Chem.*, 2016, **9**(1), 343.
18. C.S. Lehmann, N.B. Ram, I. Powis and M.H.M. Janssen, *The Journal of Chemical Physics*, 2013, **139**(23), 234307.
19. B. Ritchie, *Phys. Rev. A*, 1976, **13**(4), 1411.
20. I. Powis, *J Phys Chem A*, 2000, **104**(5), 878.
21. I. Powis, *The Journal of Chemical Physics*, 2000, **112**(1), 301.
22. A.N. Artemyev, A.D. Müller, D. Hochstuhl and P.V. Demekhin, *The Journal of Chemical Physics*, 2015, **142**(24), 244105.
23. R.E. Goetz, T.A. Isaev, B. Nikoobakht, R. Berger and C.P. Koch, *The Journal of Chemical Physics*, 2017, **146**(2), 24306.
24. N. Böwering, T. Lischke, B. Schmidtke, N. Müller, T. Khalil and U. Heinzmann, *Phys Rev Lett*, 2001, **86**(7), 1187.
25. C. Lux, M. Wollenhaupt, T. Bolze, Q. Liang, J. Köhler, C. Sarpe and T. Baumert, *Angew. Chem. Int. Ed.*, 2012, **51**(20), 5001.
26. M.M. Rafiee Fanood, N.B. Ram, C.S. Lehmann, I. Powis and M.H.M. Janssen, *Nat Commun*, 2015, **6**, 7511.
27. S. Beaulieu, A. Comby, B. Fabre, D. Descamps, A. Ferré, G. Garcia, R. Géneaux, F. Légaré, L. Nahon, S. Petit, T. Ruchon, B. Pons, V. Blanchet and Y. Mairesse, *Faraday Discuss*, 2016, **194**, 325.
28. K. Fehre, S. Eckart, M. Kunitski, C. Janke, D. Trabert, J. Rist, M. Weller, A. Hartung, L.P.H. Schmidt, T. Jahnke, R. Dörner and M. Schöffler, *J Phys Chem A*, 2019, **123**(30), 6491.
29. S. Stranges, S. Turchini, M. Alagia, G. Alberti, G. Contini, P. Decleva, G. Fronzoni, M. Stener, N. Zema and T. Prosperi, *The Journal of Chemical Physics*, 2005, **122**(24), 244303.
30. L. Nahon, G.A. Garcia and I. Powis, *Journal of Electron Spectroscopy and Related Phenomena*, 2015, **204**, 322.
31. M. Tia, M. Pitzer, G. Kastirke, J. Gatzke, H.-K. Kim, F. Trinter, J. Rist, A. Hartung, D. Trabert, J. Siebert, K. Henrichs, J. Becht, S. Zeller, H. Gassert, F. Wiegandt, R. Wallauer, A. Kuhlins, C. Schober, T. Bauer, N. Wechselberger, P. Burzynski, J. Neff, M. Weller, D. Metz, M. Kircher, M. Waitz, J.B. Williams, L.P.H. Schmidt, A.D. Müller, A. Knie, A. Hans, L. Ben Ltaief, A. Ehresmann, R. Berger, H. Fukuzawa, K. Ueda, H. Schmidt-Böcking, R. Dörner, T. Jahnke, P.V. Demekhin and M. Schöffler, *J Phys Chem Lett*, 2017, **8**(13), 2780.
32. J. Miles, D. Fernandes, A. Young, C.M.M. Bond, S.W. Crane, O. Ghafur, D. Townsend, J. Sá and J.B. Greenwood, *Anal Chim Acta*, 2017, **984**, 134.
33. A. Comby, E. Bloch, C.M.M. Bond, D. Descamps, J. Miles, S. Petit, S. Rozen, J.B. Greenwood, V. Blanchet and Y. Mairesse, *Nat Commun*, 2018, **9**(1), 5212.
34. C. Lux, M. Wollenhaupt, C. Sarpe and T. Baumert, *Chemphyschem*, 2015, **16**(1), 115.
35. W.J. Meath and E.A. Power, *Journal of Modern Optics*, 1989, **36**(7), 977.
36. D. Kröner, *J Phys Chem A*, 2011, **115**(50), 14510.
37. I. Powis, *Photoelectron Circular Dichroism in Chiral Molecules*. In: Rice SA, editor. Advances in chemical physics: Volume 139. Advances in Chemical Physics. v. 139. New York: Wiley, 2008. p. 267–329.
38. M.M. Rafiee Fanood, I. Powis and M.H.M. Janssen, *J Phys Chem A*, 2014, **118**(49), 11541.
39. J.A. Davies, J.E. LeClaire, R.E. Continetti and C.C. Hayden, *The Journal of Chemical Physics*, 1999, **111**(1), 1.
40. V. Stert, W. Radloff, C.P. Schulz and I.V. Hertel, *The European Physical Journal D - Atomic, Molecular, Optical and Plasma Physics*, 1999, **5**(1), 97.
41. A. Vredenborg, W.G. Roeterdink and M.H.M. Janssen, *Rev Sci Instrum*, 2008, **79**(6), 63108.
42. T. Baer, Booze Jon and K.-M. Weitzel, *Photoelectron Photoion Coincidence Studies of Ion Dissociation Dynamics*. In: Ng C-Y, editor. Vacuum Ultraviolet Photoionization and Photodissociation of Molecules and Clusters: WORLD SCIENTIFIC, 1991. p. 259.
43. G.A. Garcia, H. Dossmann, L. Nahon, S. Daly and I. Powis, *Phys Chem Chem Phys*, 2014, **16**(30), 16214.
44. G.A. Garcia, L. Nahon, S. Daly and I. Powis, *Nat Commun*, 2013, **4**, 2132.

View Article Online
DOI: 10.1039/D0CP01376E

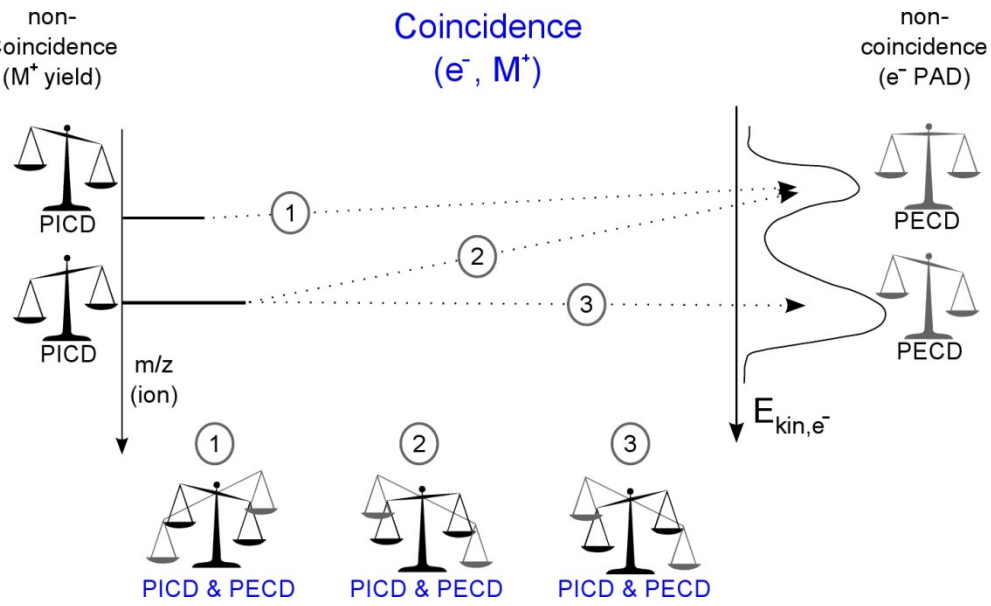

163x95mm (226 x 226 DPI)